Third Harmonic Imaging using a Pulse Inversion

Rasmussen, Joachim; Du, Yigang; Jensen, Jørgen Arendt

Published in:
Proceedings of IEEE International Ultrasonics Symposium 2011

Link to article, DOI:
10.1109/ULTSYM.2011.0563

Publication date:
2011

Document Version
Early version, also known as pre-print

Paper presented at the IEEE International Ultrasonics Symposium, Orlando Florida, 2011:

Third Harmonic Imaging using Pulse Inversion

Joachim Hee Rasmussen, Yigang Du and Jørgen Arendt Jensen

Center for Fast Ultrasound Imaging,
Biomedical Engineering group, Department of Electrical Engineering, Bldg. 349,
Technical University of Denmark, DK-2800 Kgs. Lyngby, Denmark

To be published in Proceedings of IEEE International Ultrasonics Symposium, Orlando Florida, 2011.

Third Harmonic Imaging using Pulse Inversion

Joachim Hee Rasmussen, Yigang Du and Jørgen Arendt Jensen
Center for Fast Ultrasound Imaging, Dept. of Elec. Eng. Bldg. 349,
Technical University of Denmark, DK-2800 Kgs. Lyngby, Denmark

***Abstract*—The pulse inversion (PI) technique can be utilized to separate and enhance harmonic components of a waveform for tissue harmonic imaging. While most ultrasound systems can perform pulse inversion, only few image the 3rd harmonic component. PI pulse subtraction can isolate and enhance the 3rd harmonic component for imaging on any ultrasound system capable of PI. PI was used to perform 3rd harmonic B-mode scans of a water-filled wire phantom on an experimental ultrasound system. The 3rd harmonic scans were compared to fundamental and 2nd harmonic scans on the same system. The 3rd harmonic image showed a 46% improvement in the lateral FWHM resolution compared to fundamental B-mode imaging at 75 mm depth and a 28% improvement compared to 2nd harmonic B-mode imaging. The axial FWHM resolution was improved by 35% and 30% for 3rd harmonic imaging compared to fundamental and 2nd harmonic imaging respectively. The improvements in spatial resolution and the fact that PI can isolate the 3rd harmonic suggest that it is advantageous to implement 3rd harmonic imaging on ultrasound systems capable of PI.**

I. Introduction

Tissue harmonic imaging is a technique widely used in commercial ultrasound systems to improve spatial resolution. In harmonic B-mode imaging, however, an overlap is often seen between the harmonic components in the received RF signal, making separation of a single harmonic band difficult. The harmonics are often hidden in the spectrum by overlaps between neighboring harmonics, sum and difference harmonics, and noise. Contributions from neighboring harmonics could therefore, be included in the harmonic B-mode image even after filtration, thus degrading the spatial resolution of the final harmonic image. Pulse inversion (PI) [1][2] can be used to suppress the neighboring harmonic components for a more efficient isolation of a specific harmonic. Ultrasound systems today employ PI but use this often only to image the 2nd harmonic component. PI however, is fully capable of isolating the 3rd harmonic component on the ultrasound system. The purpose of this paper is to perform 3rd harmonic imaging on an ultrasound system capable of PI and investigate whether 3rd harmonic imaging is advantageous over 2nd harmonic and fundamental imaging.

II. Theory

A. Pulse Inversion

A PI technique can be used to isolate and enhance the 2nd and 3rd harmonics from their neighboring harmonic components. In this technique two pulses (regular pulse, 180° phase shifted pulse) are transmitted in turn. While a 180° phase shift can be detected for the fundamental component of the received signal a corresponding 360° and 540° phase shift can be seen for the 2nd and 3rd harmonic components respectively [3][4]. To suppress the odd order harmonics each correlated pair (regular and phase shifted) of the received responses are summed. Harmonic components that are in phase (all even harmonics) will double in amplitude, while out of phase components (all odd harmonics) will cancel out (see Fig. 1). This separates and enhances the 2nd harmonic component, which in turn then can be filtered and used for imaging. To suppress the even order harmonics the pairs of received responses are subtracted, thus causing all odd harmonics to double in amplitude and even harmonics to cancel out. In this manner the 3rd harmonic component can be isolated and enhanced for imaging.

B. Waveform Bandwidth

The bandwidth of the transmitted pulse can also be used to reduce overlap between the harmonic components. When transmitting a pulse with a narrow bandwidth the harmonic components are more easily separable compared to wide bandwidth transmit waveforms [4][5]. The disadvantage in using narrow bandwidth waveforms is that the axial resolution is reduced [3][6]. The task is therefore, to weight the importance of a good separation of harmonics over changes in axial resolution when selecting a waveform bandwidth.

III. Experimental Setup

A B-mode scan of a wire phantom is performed by PI on an experimental synthetic aperture real-time ultrasound system (SARUS) [7][8]. This scanner is capable of performing PI and 2nd harmonic imaging [9] and is therefore also capable of performing 3rd harmonic imaging. SARUS is used to record raw channel data from a commercially available 192 element convex transducer (BK8820e). Images are made for purely linear B-mode, 2nd harmonic B-mode, and 3rd harmonic B-mode of a water filled wire phantom. The phantom contains 6 equidistant wires spaced 25 mm apart. The transducer is held in a fixed position centered over the wires in the phantom with the surface of the transducer slightly submerged in water. Sixty-five active channels in a sliding aperture are used for transmit and 192 channels for receive. Apodization in both transmit and receive is set to be a Hamming function. A fixed focal depth of 65 mm is used - this is also the elevation focus of the convex transducer. For each position of the aperture two emissions, one regular and one inverted are performed. In total 32 dual emissions are recorded for each frame in

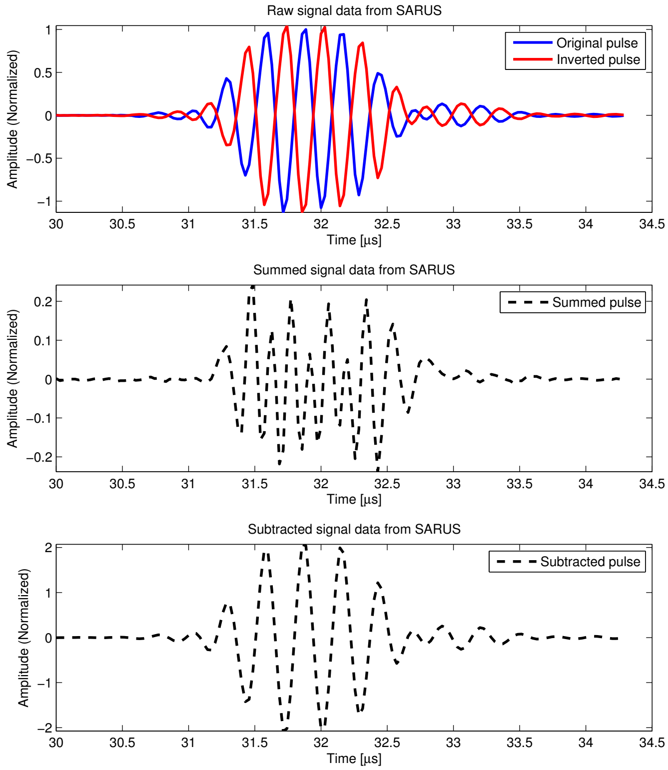

Figure 1. Data received from SARUS. Top plot shows the received pulses (normal and inverted). Middle plot shows the resulting pulse after pulse summation. Bottom plot shows the resulting pulse after pulse subtraction. All data have been normalized to the original pulse in the top plot.

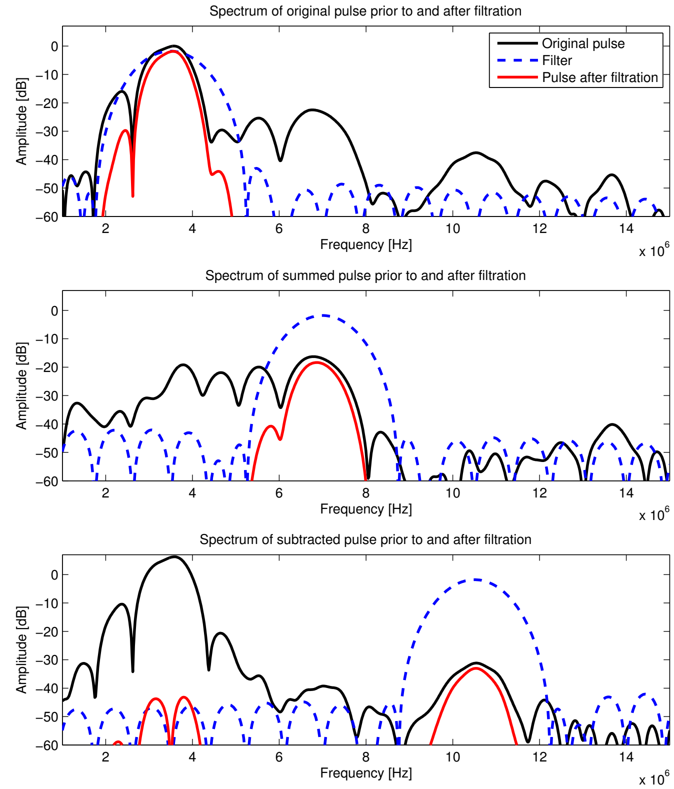

Figure 2. Spectrum of received RF signals. Top figure shows the spectrum of the fundamental signal prior to and after matched filtration. Middle shows the summed pulse used for 2nd harmonic imaging before and after filtration. Bottom figure shows the subtracted pulse used in 3rd harmonic imaging before and after matched filtering.

the image. The collection of data in a frame can be used for two regular B-mode images (one for the regular pulse; one also for the inverted pulse), one 2nd harmonic B-mode image (from the summed pulse), and one 3rd harmonic B-mode image (from the subtracted pulse). The Full Width at Half Maximum (FWHM (-6 dB)) and the Full Width at One Tenth Maximum (FWOTM (-20 dB)) values of the scatterers in the image are measured for fundamental, 2nd harmonic, and 3rd harmonic imaging and the values are compared.

Since the transducer of the system only has a limited 2-way frequency response the center frequency of the transmitted signal must be chosen such that it allows for the detection of both the 2nd and 3rd harmonic component in the received signal. On the other hand, the center frequency must also be chosen such that the transducer is able to transmit enough energy to induce the non-linear response. In this case a center frequency of 3.5 MHz for the 4 cycle excitation pulse is set. This means that the 2nd and 3rd harmonic components will be found at 7 MHz and 10.5 MHz respectively. All data is filtered using a matched filter having the same peak frequency as the harmonic component at hand. Image data is then beamformed using the Beamformation Toolbox 3 (BFT3) [10].

IV. Results

The amplitude spectrum of the received waveforms in Fig. 2 shows the harmonic components in the original pulse at 3.5 MHz, 7 MHz, and 10.5 MHz as predicted. The pulse summation reduces the fundamental and 3rd harmonic components and enhances the 2nd harmonic component. The pulse subtraction reduces the 2nd harmonic while enhancing the fundamental and 3rd components. The blue dashed line in Fig. 2 shows the amplitude of the matched filter used to separate the harmonic component.

Fig. 3 shows the 3rd harmonic B-mode image of the first 4 wires of the phantom after scanline conversion. Because only a fraction of the transmitted energy is converted into 3rd harmonic energy, the signal to noise ratio (SNR) is low compared to e.g. fundamental B-mode imaging [6]. However, in spite of the lower SNR the 4 wires are clearly seen in the B-mode image. Fig. 4 shows the point spread functions (PSF) of the linear, 2nd, and 3rd harmonic components for the 3rd wire in the phantom (at 75 mm depth). From this plot it is seen that the side lobe energy decreases for 2nd and 3rd harmonic imaging and that the main lobe of the PSF is much narrower for the harmonic components compared to the fundamental component. The FWHM and FWOTM values for the first 3 wires in the phantom are measured and shown in Table I and Table II. The tables show that lateral FWHM for

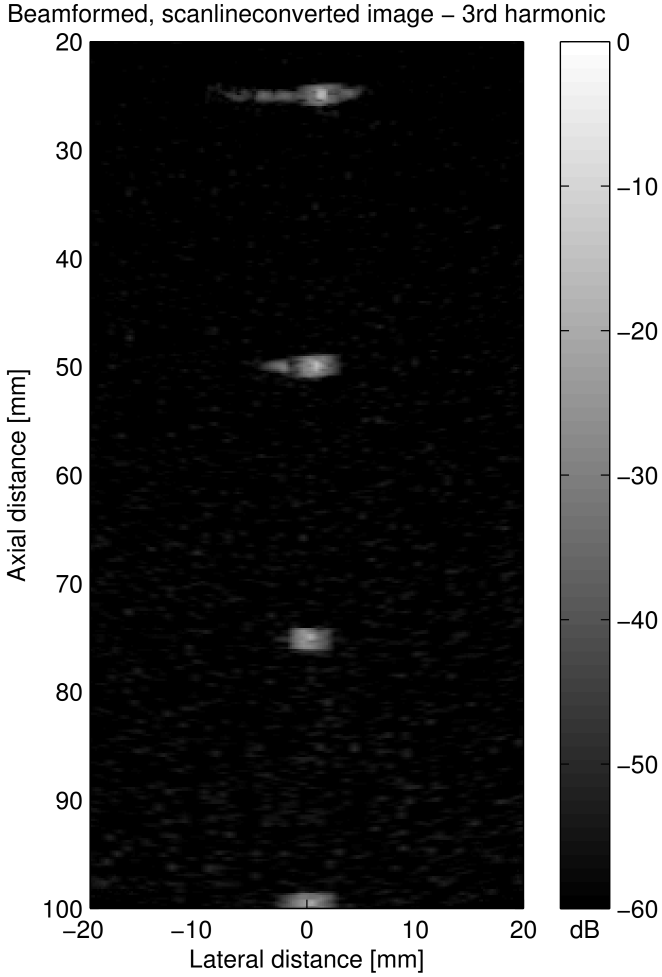

Figure 3. 3rd harmonic B-mode image of the wire phantom using the convex transducer. The image has 60 dB dynamic range.

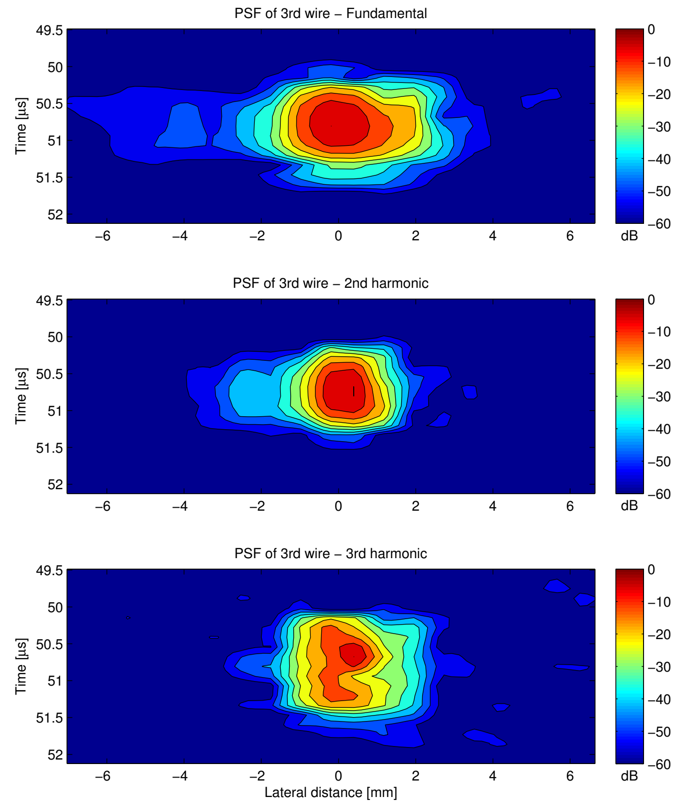

Figure 4. The point spread functions (PSF) of the fundamental pulse (top), 2nd harmonic pulse (middle), and 3rd harmonic pulse (bottom). The PSFs are displayed with 6dB contour lines.

Table I
FWHM VALUES FOR WIRES AT 25 MM, 50 MM, AND 75 MM DEPTH.

Depth	Direction	Fundamental	2nd harmonic	3rd harmonic
25 mm	Lateral [mm]	2.19	1.25	0.86
	Axial [mm]	0.94	0.86	0.98
50 mm	Lateral [mm]	2.70	1.21	0.70
	Axial [mm]	0.94	0.94	1.02
75 mm	Lateral [mm]	2.03	1.52	1.09
	Axial [mm]	1.02	0.94	0.66

Table II
FWOTM VALUES FOR WIRES AT 25 MM, 50 MM, AND 75 MM DEPTH.

Depth	Direction	Fundamental	2nd harmonic	3rd harmonic
25 mm	Lateral [mm]	4.22	2.19	1.72
	Axial [mm]	1.48	1.29	2.54
50 mm	Lateral [mm]	4.61	2.07	3.24
	Axial [mm]	1.45	1.41	1.99
75 mm	Lateral [mm]	4.53	2.46	3.40
	Axial [mm]	1.48	1.48	2.34

the 3rd harmonic component is lower than FWHM for both fundamental and 2nd harmonic components. Third harmonic axial FWHM is only reduced for the 3rd wire in the phantom. The lateral FWOTM values for the 3rd harmonic component are lower than those for the fundamental component but only the value for the first wire is lower than the value of the 2nd harmonic component. For the axial FWOTM values the 3rd harmonic component shows no improvement compared to the other imaging methods.

V. DISCUSSION

The reduction in the FWHM and FWOTM values seen for the harmonic components in Table I and Table II show that the spatial resolution is improved. There is a 46% reduction in the lateral FWHM resolution between the fundamental and 3rd harmonic components at 75 mm depth and a 28% reduction in the lateral FWHM resolution between the 2nd and 3rd harmonic components at that same depth. The axial FWHM resolution for the 3rd harmonic component is reduced by 35% and 30% compared to the fundamental and 2nd harmonic components respectively. The increase in 3rd harmonic axial FWOTM results from the bandwidth of the matched filter that is used prior to imaging. It is necessary to choose a filter with a bandwidth that is capable of isolating the individual harmonics while still attaining a low axial resolution. In this specific case the bandwidth of the filter was chosen such that there was no harmonic overlap between the 2nd and 3rd harmonics and the axial FWHM resolution changed as little as possible compared to fundamental and 2nd harmonic axial FWHM resolution.

Since the results show that 3rd harmonic imaging does improve the lateral resolution compared to both fundamental and 2nd harmonic imaging, it could prove advantageous to implement 3rd harmonic imaging on ultrasound systems capable of PI. The only changes needed on the 2nd harmonic PI systems is a pulse subtraction technique. By this simple method the system could perform both 2nd and 3rd harmonic imaging from the same set of RF data.

While harmonic imaging using PI has the benefits of improved spatial resolution and low side lobes, PI also has some drawbacks. First of all, two emissions need to be received for every image line to derive the summed and subtracted pulses used in PI. This reduces the frame rate of the imaging system by a factor of 2 compared to linear B-mode imaging. The dual emissions also increase the amount of data the processor of the imaging system must be able to handle without further loosing frame rate. The loss of frame rate could prove very disadvantageous, if the scan is made on non-stationary tissues. Here any tissue motion may lead to a phase change in the paired received signals and severely reduce the harmonic components of the summed and subtracted pulses. Secondly, the transducer must function optimally over a broad spectrum to be able to transmit and receive a maximum energy at the fundamental, 2nd harmonic, and 3rd harmonic center frequency. If there is an energy loss at either frequencies the signal to noise ratio (SNR) in the image will radically decrease reducing the penetration depth of the harmonic component. Since the attenuation of the harmonic components also is much higher than that of the fundamental component the importance of selecting the optimal center frequency is imperative.

VI. Conclusion

Third harmonic B-mode imaging has successfully been accomplished using SARUS. The lateral resolution of the 3rd harmonic image is determined to be higher than that of 2nd harmonic and fundamental B-mode imaging.

VII. Acknowledgements

This work was supported by grant 024-2008-3 from the Danish Advanced Technology Foundation and BK Medical Aps, Denmark.

References

[1] C. S. Chapman and J. C. Lazenby, “Ultrasound imaging system employing phase inversion subtraction to enhance the image,” *US Patent*, vol. 5632277, 1997.

[2] D. H. Simpson, C. T. Chin, and P. N. Burns, “Pulse inversion Doppler: a new method for detecting nonlinear echoes from microbubble contrast agents,” *IEEE Trans. Ultrason., Ferroelec., Freq. Contr.*, vol. 46, no. 2, pp. 372–382, 1999.

[3] J. A. Jensen, “Medical ultrasound imaging,” *Progress in Biophysics and Molecular Biology*, vol. 93, pp. 153–165, 2007.

[4] M. A. Averkiou, “Tissue harmonic imaging,” in *Proc. IEEE Ultrason. Symp.*, vol. 2, 2000, pp. 1563–1572.

[5] C. Shen and P. Li, “Harmonic leakage and image quality degradation in tissue harmonic imaging,” *IEEE Trans. Ultrason., Ferroelec., Freq. Contr.*, vol. 48, pp. 728–736, 2001.

[6] A. Bouakaz and N. de Jong, “Native tissue imaging at superharmonic frequencies,” *IEEE Trans. Ultrason., Ferroelec., Freq. Contr.*, vol. 50, pp. 496–506, 2003.

[7] J. A. Jensen, M. Hansen, B. G. Tomov, S. I. Nikolov, and H. Holten-Lund, “System architecture of an experimental synthetic aperture real time ultrasound system,” in *Proc. IEEE Ultrason. Symp.*, Oct. 2007, pp. 636–640.

[8] J. A. Jensen, H. Holten-Lund, R. T. Nielson, B. G. Tomov, M. B. Stuart, S. I. Nikolov, M. Hansen, and U. D. Larsen, “Performance of SARUS: A Synthetic Aperture Real-time Ultrasound System,” in *Proc. IEEE Ultrason. Symp.*, Oct. 2010, pp. 305–309.

[9] J. Rasmussen, Y. Du, and J. A. Jensen, “Non-linear imaging using an experimantal synthetic aperture real time ultrasound scanner,” *IFMBE Proceedings*, vol. 34, pp. 101–104, 2011.

[10] J. M. Hansen, M. C. Hemmsen, and J. A. Jensen, “An object-oriented multi-threaded software beam formation toolbox,” in *Proc. SPIE - Medical Imaging - Ultrasonic Imaging and Signal Processsing*, vol. 7968, 2011, p. 79680Y.